Triplet Phenylarsinidene and Its Oxidation to Dioxophenylarsine

Weiyu Qian[1], Peter R. Schreiner[1], and Artur Mardyukov[1]*

Affiliations: [1]Institute of Organic Chemistry, Justus Liebig University, Giessen, Germany
*Correspondence to: artur.mardyukov@org.chemie.uni-giessen.de

Abstract: Diradicals are key intermediates involved in numerous chemical processes and have attracted considerable attention in synthetic chemistry, biochemistry, and materials science. Even though parent arsinidene (H–As) has been characterized well, the high reactivity of subsituted arsinidenes has prohibited their isolation and characterization to date. Here, we report the preparation of triplet phenylarsinidene through the photolysis of phenylarsenic diazide, isolated in an argon matrix, and its subsequent characterization by infrared and UV/Vis spectroscopy. Doping the matrices containing phenylarsinidene with molecular oxygen leads to the formation of hitherto unknown *anti*-dioxyphenylarsine. The latter undergoes isomerization to novel dioxophenylarsine upon 465 nm irradiation. The assignments were validated by isotope-labeling experiments combined with B3LYP/def2-TZVP computations.

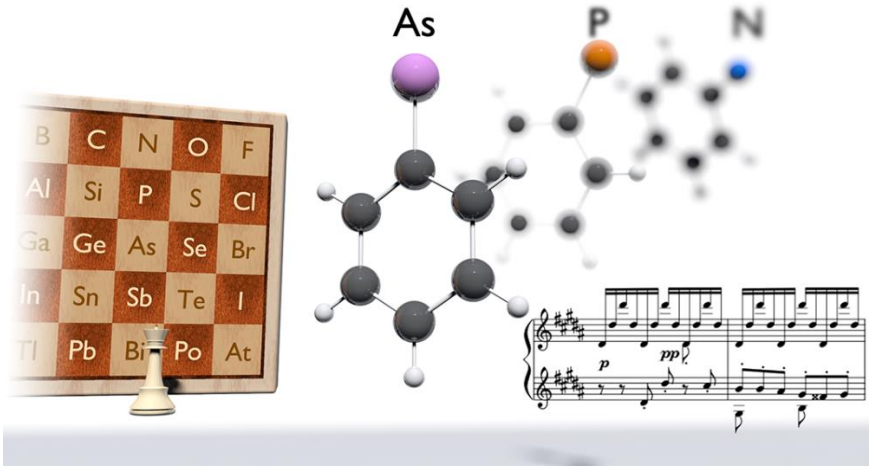

Keywords: Arsinidene, Matrix Isolation, Reactive Intermediates, Photochemistry

Main Text:

Owing to their important roles as versatile reagents and pivotal intermediates in numerous chemical processes, the properties and reactivity of carbenes (R–C–R)[1-3] and nitrenes (R–N)[4-6] have been extensively studied, despite their high reactivity and instability. However, there are still many families of reactive intermediates that have eluded isolation and spectroscopic identification. Among these are arsinidenes (R–As), the neutral monovalent arsenic congeners of nitrenes (R–N), and phosphinidenes (R–P) with six electrons in their valence shell. Depending on the nature of the R-substituent they may adopt either a singlet or a triplet electronic ground state (Scheme 1A). Several attempts have been made to prepare free arsinidenes, but the detection and identification of these species has been hampered by their instability and fleeting existence.[7,8] To date, only electronic and vibrational transitions of parent arsinidene (H–As) have been studied by flash photolysis of AsH_3.[9-12] All other evidence for the existence of arsinidenes was derived from trapping and complexation experiments. For example, several terminal arsinidene complexes with transition metals were synthesized and structurally characterized by X-ray crystal structure analysis.[13-17] Furthermore, the *N*-heterocyclic-carbenes (NHCs)[18,19] and *N*-heterocyclic silylenes (NHSis)[20] were also utilized for the stabilization of arsinidenes. In addition, HM=AsH (M = Ti, Zr, Hf) complexes were prepared by the reaction of group IV metal atoms with AsH_3 under matrix isolation conditions.[21] The arsaketene radical and anion were trapped in a cryogenic matrix by reaction of laser-ablated arsenic atoms with carbon monoxide.[22]

Phenylarsinidene (**1**), the heavier analogue of phenylphosphinidene (PhP), is deemed to be a key intermediate for the synthesis of arsol-containing compounds in organic electronics[23] and as a ligand for the stabilization of isolable alumenenes.[24] Arsphenamine, also known under its trade name Salvarsan, the first modern antimicrobial agent, may be regarded as the trimer of an aryl arsinidene, which was synthesized from 3-nitro-4-hydroxyphenylarsonic acid.[25] Diarsenes (R-As=As-R), the arsinidene dimers, can be quantitatively obtained *in situ* from thermolysis of arsa-Wittig reagents in solution.[26,27]

In contrast to the unknown arsinidenes, several “free” phosphinidenes have been isolated under matrix isolation conditions and characterized by IR, UV/Vis, and EPR spectroscopy, which includes the parent phosphinidene (HP),[28] methoxyphosphinidene (CH_3OP),[29] phenylphosphinidene (PhP),[30,31] mesitylphosphinidene (MesP),[32,33] and ethynylphosphinidene (HCCP)[34] that have triplet electronic ground states. It has also been experimentally shown that strong π-donor substitution (e.g., R_2N–, R_2P–) stabilizes the singlet state of phosphinidene over the triplet.[35,36] To date, however, there is no clear experimental evidence confirming the formation of uncomplexed alkyl- and aryl-arsinidenes, and their reactivity is unknown. Herein, we report the first synthesis as well as IR and UV/Vis spectroscopic characterization of phenylarsinidene **1**, and its oxidation to *anti*-dioxyphenylarsine (**3a**) and dioxophenylarsine (**5**) through the reaction of **1** with molecular oxygen (O_2) and subsequent trapping in argon matrices at 10 K (Scheme 1B).

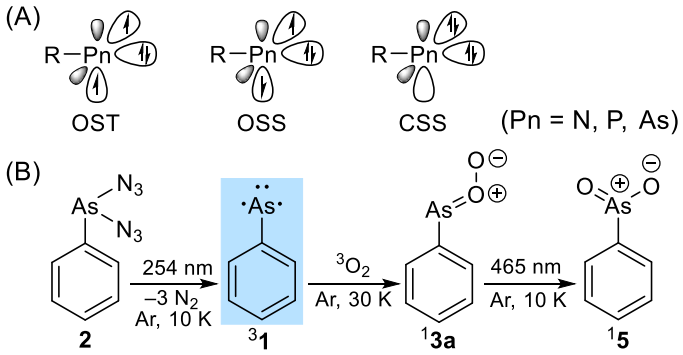

Scheme 1. (A) Common electronic configurations of pnictinidenes (OST – open shell triplet; OSS – open-shell singlet; CSS – close-shell singlet). (B) Photochemical generation of phenylarsinidene **1** and subsequent (photo)reactivity.

Results and Disscusion:

It has recently been shown that transient phosphorus species can be readily generated by the thermal and photochemical N_2 extrusion from the corresponding azides.[29,37,38] Our strategy for the preparation of **1** was the photolysis of phenylarsenic diazide (**2**) in the reaction **2** $\rightarrow$ **1** + 3 N_2 (N_2 as the IR invisible byproduct). Diazide **2** was synthesized from the corresponding dichloride precursor (for synthetic details see the Supplementary Materials). The matrix-isolated IR spectrum of **2** shows two strong bands at 2109.9 and 2086.7 cm^{-1}, which were assigned as symmetric and asymmetric NNN stretching modes, respectively. In addition, two medium-intensity IR bands at 1240.5 and 1219.2 cm^{-1} could be tentatively assigned to the interior N=N symmetric and asymmetric stretching modes of **2**. Irradiation of matrices containing **2** with light λ = 254 nm results in the rapid disappearance of its IR bands and simultaneously a new set of IR bands appears at 1575, 1473, 1429, 1325, 1065, 1024, 994, 904, 731, 687, and 426 cm^{-1} (Figure 1b). The excellent agreement between experimentally observed and computed IR spectrum at B3LYP/def2-TZVP is taken as evidence for the formation of triplet **1** (^{3}**1**, Table S1). For example, the strong IR bands at 731 and 687 cm^{-1} are attributed to the C–H out-of-plane (o.o.p.) vibrational modes. At the B3LYP/def2-TZVP level of theory, the C–As stretch shows a frequency of 295 cm^{-1}, which is, unfortunately, at the lower limit of our IR spectrometer, and therefore cannot be detected.

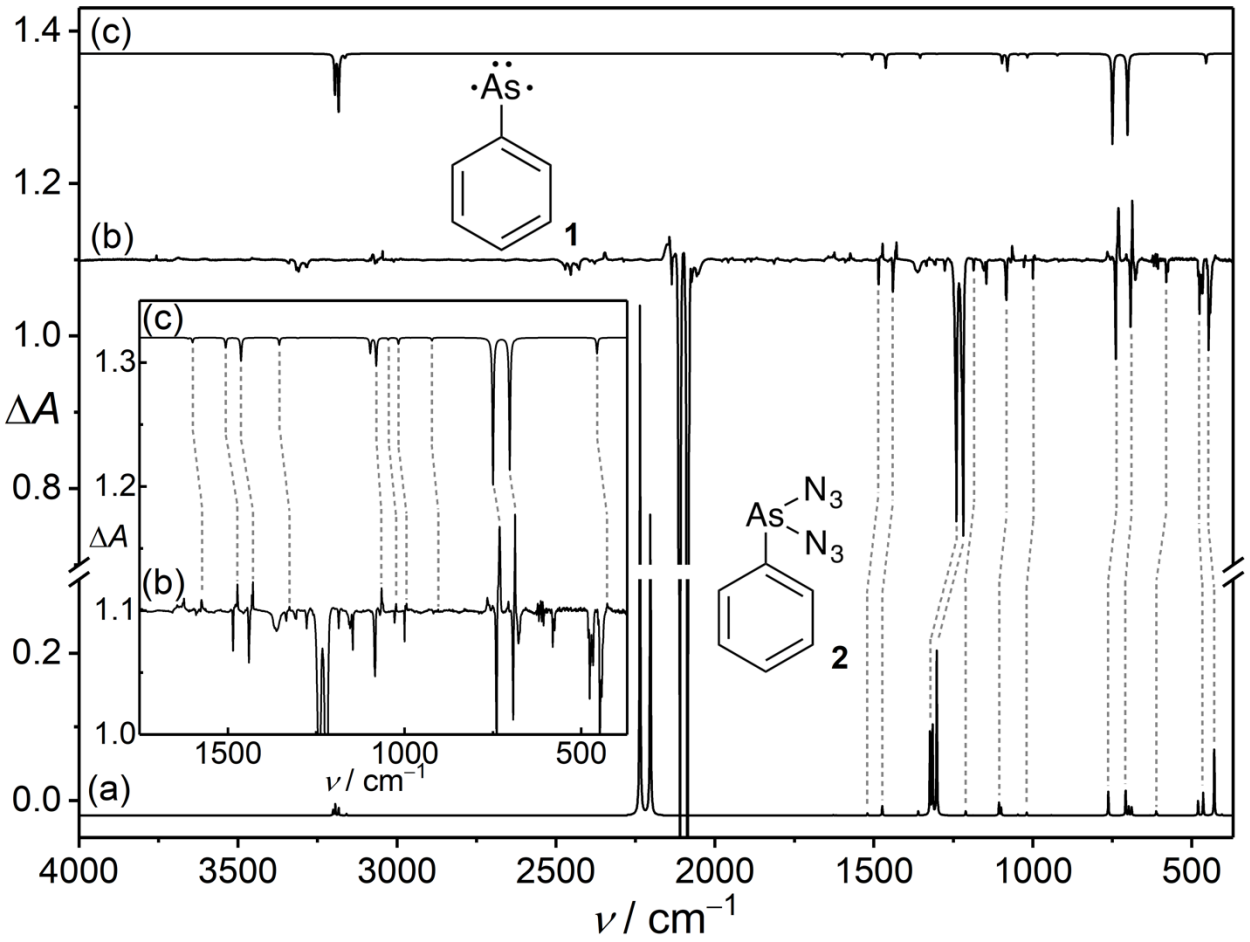

Figure 1. (a) Unscaled computed spectrum for ^{3}**1** at B3LYP/def2-TZVP. (b) IR difference spectrum shows the changes upon 5 min 254 nm irradiation. (c) Unscaled computed spectrum for **2** at B3LYP/def2-TZVP. Inset: Expanded spectra for detail display in the range of 1750-400 cm^{-1}.

The UV/Vis spectral analysis of **2** shows intensive absorptions in the UV region, which includes strong transition bands at 192, 218, and 272 nm (Figure 2). They completely vanish after 2 min of 254 nm irradiation, and simultaneously the strong absorption band of ^{3}**1** at 262 nm together with weak bands at 280 nm and 342 nm appear. The UV/Vis spectrum of ^{3}**1** qualitatively resembles the spectra of phenylphosphinidene in an argon matrix.[30] The experimental UV/Vis spectrum of ^{3}**1** agrees well with the intense electronic absorptions at 277 and 296 nm (f = 0.128 and 0.086), as well as medium absorptions at 343 and 375 nm (f = 0.007 and 0.009) computed at TD-B3LYP/def2-TZVP.

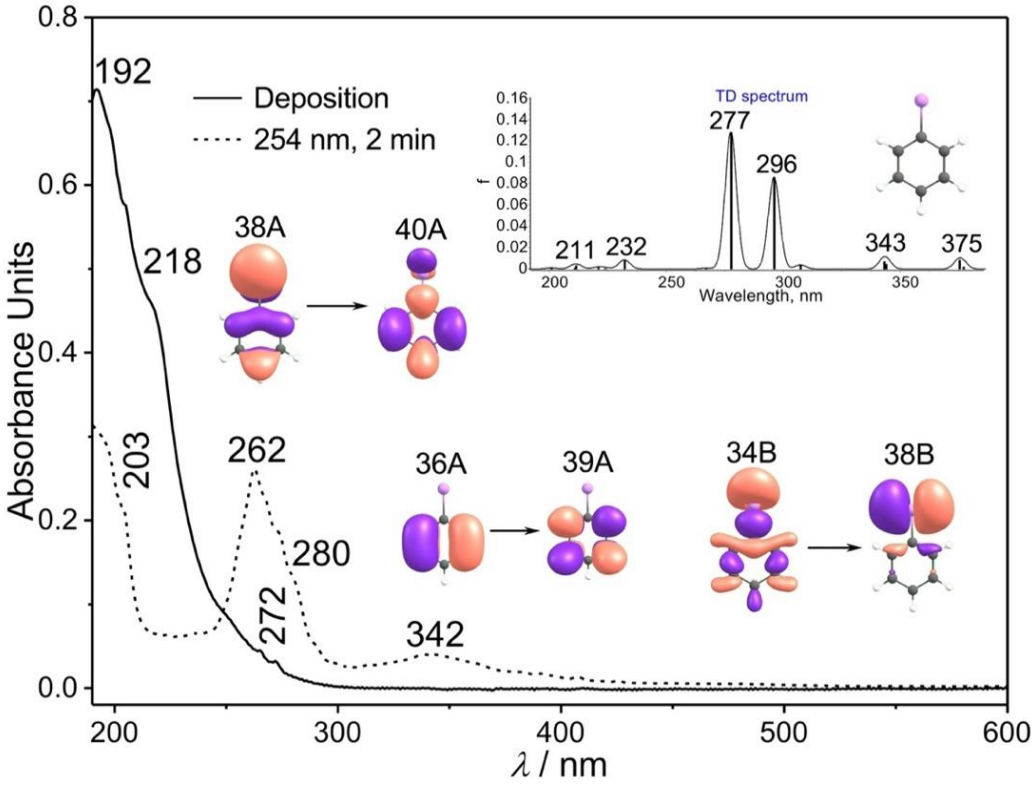

Figure 2. Solid line: UV/Vis spectrum of **2** isolated in argon (10 K). Dashed line: UV/Vis spectrum of ^{3}**1** at 10 K: the photochemistry of **2** after irradiation at λ = 254 nm in argon at 10 K. Inset: Computed [TD-B3LYP/def2-TZVP] electronic transitions for ^{3}**1**.

According to our B3LYP/def2-TVZP computations, **1** shows planar C_{2v} symmetry with an electronic $^3A_2$ ground state. Arsinidene **1** has a large singlet-triplet energy separation of ΔE_{ST}= 22.2 kcal mol^{-1} at B3LYP/def2-TZVP and 25.0 kcal mol^{-1} at CASSCF(8,8)/cc-pVDZ underscoring its triplet electronic ground state nature, similar to phenylphosphinidene (**6**) (ΔE_{ST}= 33.0 kcal mol^{-1} at B3LYP/def2-TZVP; ΔE_{ST}= 24.3 kcal mol^{-1} at CASSCF(8,8)/cc-pVDZ) and phenylnitrene (**7**) (ΔE_{ST}= 30.0 kcal mol^{-1} at B3LYP/def2-TZVP; ΔE_{ST}= 17.3 kcal mol^{-1} at CASSCF(8,8)/cc-pVDZ). We have also compared key geometric parameters of **1** with **6** and **7**. The optimized structures are presented in Figure S1. As expected, the C–As bond length of **1** is considerably longer (1.932 Å) than C–P (1.791 Å) and C–N (1.318 Å) of **6** and **7**, respectively. Moreover, there are slight differences between the C=C bonds of the phenyl rings. In the case of **6** and **7**, the benzene rings show more bond alternation than in **1**. This implies that there is almost no delocalization of spin density for the arsenic atom into the phenyl ring, probably owing to a mismatch of the orbital sizes: 2p (C) overlap with the 4p (As). This is in line with computed spin densities: a higher positive spin density resides at the arsenic atom of 1.95 in **1** compared to nitrogen (1.57) in **6** and phosphorus (1.88) in **7** (Figure S1). The computed T_1 diagnostic values for **1** (0.036, Supplementary Materials), **6** (0.040), and **7** (0.039) exceed the historic criteria $T_1 \leq 0.02$ for main group species,[39] which suggests that single-reference methods are likely not reliable for this system. Therefore, the geometry optimizations were also carried out at the CASSCF(8,8)/cc-pVDZ level of theory (Figure S1), which shows the same trend of the structural characteristics of **1**, **6,** and **7**. The thermodynamic stability of **1** over **6** and **7** is also evident by the

sizable reaction enthalpy of the homodesmotic equation (1): ΔH_r = 75.3 kcal mol^{-1} X = As, 63.9 kcal mol^{-1} X = P, 39.1 kcal mol^{-1} X = N.

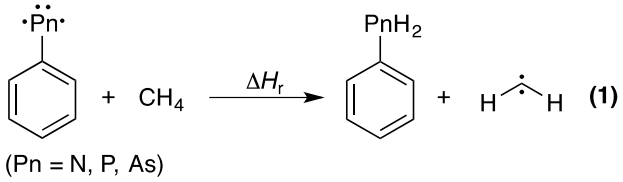

The preparation and matrix isolation of ^{3}**1** also enables us to investigate its reaction with molecular oxygen ($^3O_2$) that may lead to the formation dioxophenylarsine ($PhAsO_2$, **5**), a novel compound, which is a hitherto unknown arsenic analogue of nitrobenzene. Previously, Sander *et al.* demonstrated that the reaction of **7** with $^3O_2$ in xenon matrices yields the most stable *syn*-phenylnitroso oxide as an intermediate product, which isomerizes to nitrobenzene upon 460 nm irradiation.[40] We also reported the oxidation of **6**, where we detected only cyclic 3-phenyl-1,2,3-dioxaphosphirane.[30] Similar to the nitrogen analogue, the latter rearranges into phenyldioxophosphorane upon selective irradiation (Scheme 2).

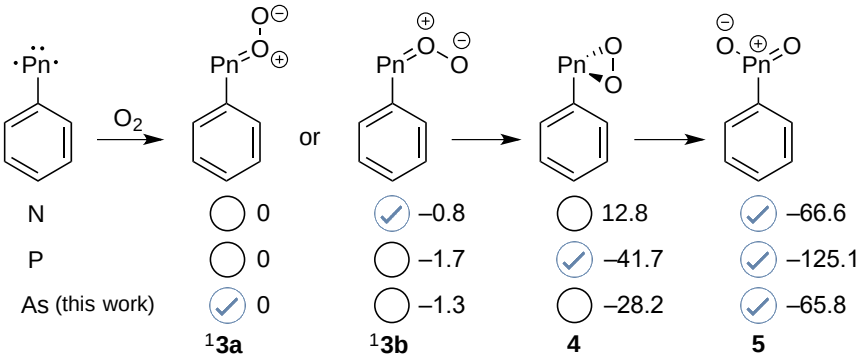

Scheme 2. Summary of the reactions of phenyl pnicitinidenes with molecular oxygen. Relative energies (in kcal mol^{-1}) computed at B3LYP/def2-TZVP.

Doping argon matrices containing **2** with variable oxygen concentrations in the range of 0.1–1% and subsequent photolysis at 254 nm showed no changes in the IR spectrum; only **1** was observed. However, after annealing the matrix at 35 K for 5 min, a group of new peaks at 1478.3, 1434.2/1436.2, 1331.6. 1160.4, 1049.2, 1031.7, 993.5, 735.7, and 687.2 cm^{-1} appeared gradually (Figure S2). For example, a strong peak at 1031.8 cm^{-1} can be attributed to the O–O stretching vibration and its position is quite close to that in *syn*-phenylnitroso oxide (1000 and 990 cm^{-1}, Xe-matrix).[40] By comparison with computed infrared vibrations for all potential candidates, this set of bands was assigned to *anti*-phenyldioxylarsinene (**3a**). The assignment of **3a** is further corroborated by ^{18}O-labeling experiments. For example, the O–O stretching vibration in **3a** is computed to have a 59.0 cm^{-1} red shift, which is in good accordance with the experimental shift of 59.6 cm^{-1}. However, because arsenic is less conjugated to the phenyl ring and much heavier than phosphorus and nitrogen, the other bands associated with the phenyl motif are barely disturbed upon isotope labeling (Table S2). We also found that **3a** is photolabile when exposed to 465 nm light. The IR bands of **3a** vanish rapidly and a new group of peaks at 1490.4, 1447.4/1440.4, 1315.8, 1084.1, 1075.5, 1016.8, 923.2, 741.6, and 684.7 cm^{-1} appear contemporarily (Figure 3). The experimentally observed IR

spectrum agrees well with the computed spectrum of dioxophenylarsine **5**. The strong IR bands at 1016.8 and 923.2 cm^{-1} are due to the OAsO asymmetric and symmetric stretching modes, respectively. They show large shifts of 42.0 and 47.6 cm^{-1} in the ^{18}O-labeling experiment, which match nicely with computed shifts of 43.1 and 48.5 cm^{-1}, respectively (Table S3).

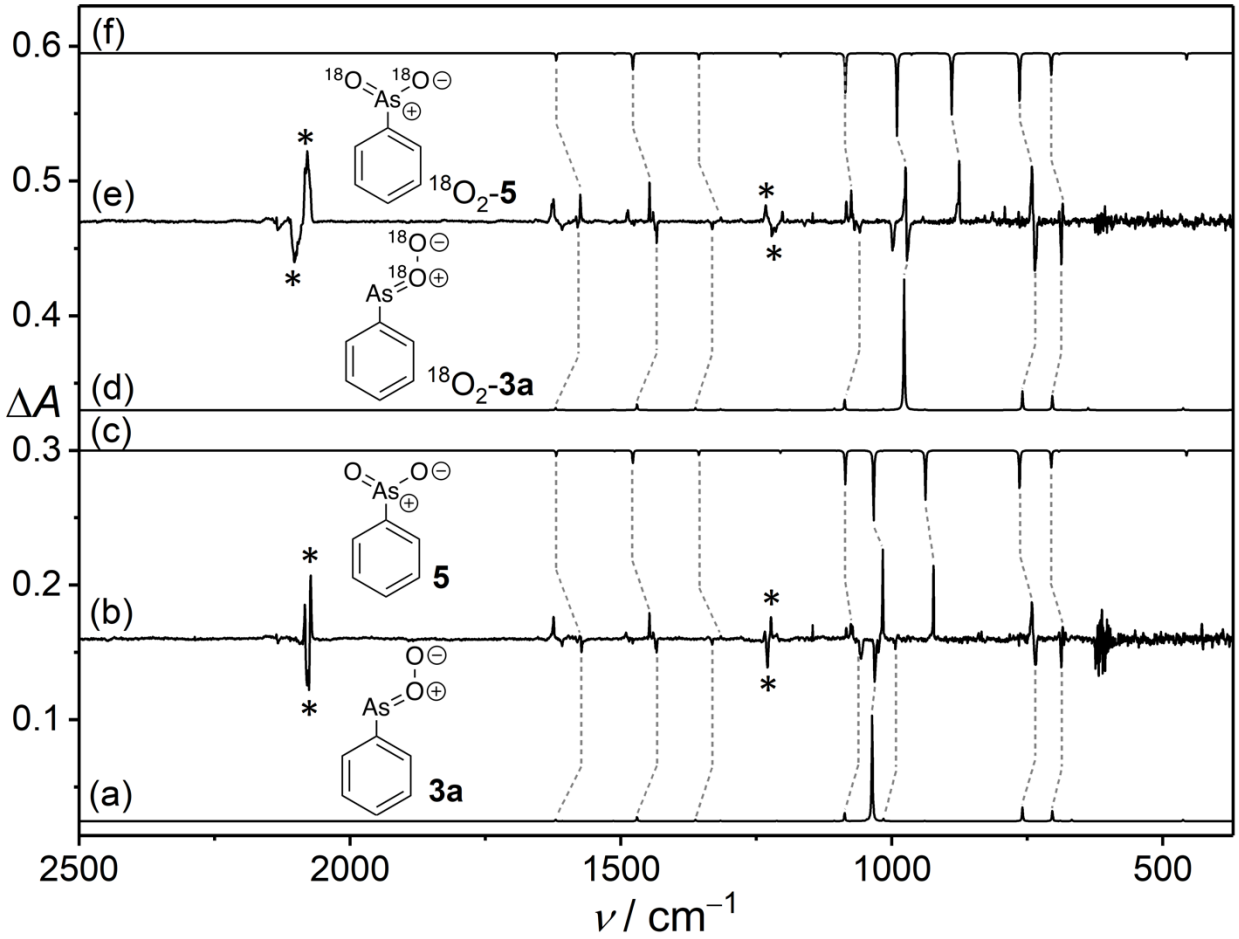

Figure 3. (a) Unscaled computed spectrum for **3a** at B3LYP/def2-TZVP. (b) IR difference spectrum shows the changes upon 1 min 465 nm irradiation of 1% O_2 doped Ar-matrix. (c) Unscaled computed spectrum for **5** at B3LYP/def2-TZVP. (d) Unscaled computed spectrum for $^{18}O_2$-**3a** at the B3LYP/def2-TZVP levels. (e) IR difference spectrum shows the changes upon 1 min 465 nm irradiation of 1% $^{18}O_2$ doped Ar-matrix. (f) Unscaled computed spectrum for $^{18}O_2$-**5** at B3LYP/def2-TZVP. The matrix sites of unreacted **2** are depicted as (*).

The reaction of **1** with O_2 was also monitored by UV/Vis spectroscopy. The transition bands of **1** disappear upon annealing at 35 K for several minutes, and simultaneously transitions at 192 and 218 nm (strong), 261 nm (moderate), and 478 nm (weak, broad) (Figure S3, solid line) appear. All new bands correlate well with the values of the electronic excitations of **3a** at 198 nm (*f* = 0.076), 260 nm (*f* = 0.163), and 456 nm (*f* = 0.158) computed at TD-B3LYP/def2-TZVP. Further irradiation at 465 nm results in the disappearance of the broad band at 478 nm and the formation of **5**.

We undertook a detailed computational analysis of the reaction of **1** with O_2 (Figure 4). The absence of characteristic bands of **3a** before annealing, even at a high O_2 concentration (> 2%) implies that the reaction between **1** and O_2 has an activation barrier. Note that the reaction mechanism of **1** with O_2 on the triplet surface from ^{3}**1** to ^{3}**3a** is slightly endothermic, followed by intersystem crossing (ISC) to the ^{1}**3a**. Alternatively, the formation of ^{1}**3a** may happen through crossing of the triplet to singlet potential energy surface, which occurs at the minimum energy crossing point (MECP) at –9.2 kcal mol^{-1}. Additionally, the energy of MECP of **3b** (–5.9 kcal mol^{-1}) is higher than that of ^{1}**3a**, thus making the formation of **3b** unfavorable. Interestingly, Sander and co-workers reported that the reaction of phenylnitrene **6** with O_2 results in the formation of *syn*-phenylnitroso oxide, which is thermodynamically more stable that the *anti*-conformer (Scheme 2).[40] In our experiments, the *anti*-conformer **3a** formed exclusively, which is 1.3 kcal mol^{-1} (B3LYP/def2-TZVP) less stable than the *syn*-conformer **3b** with a rotamerisation barrier of 17.9 kcal mol^{-1}. The tautomerization of **3a** to 3-phenyl-1,2,3-dioxaarsirane (**4**) proceeds with a barrier of 6.8 kcal mol^{-1}. The subsequent rearrangement of **4** to **5** is associated with a barrier of 37.7 kcal mol^{-1}. Although we did not observe **4** spectroscopically, this was to be expected, since the conversion of **3a** to **5** through **4** can only be accomplished via photoexcitation. According to TD-B3LYP/def2-TZVP computations, **4** has an electronic transition at 383 nm (f = 0.011) (Figure S4), which suggests the intermediacy of this highly labile species upon irradiation.

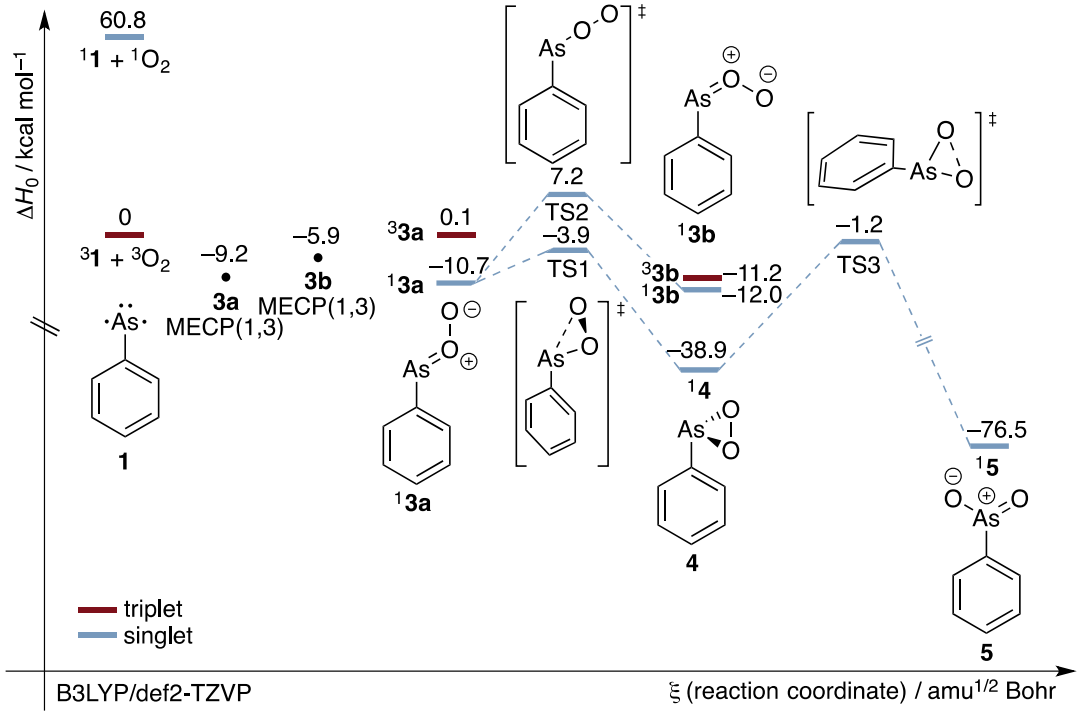

Figure 4. Potential energy profile (ΔH_0, kcal mol^{-1}) of the reactions of ^{3}**1** with molecular oxygen at B3LYP/def2-TZVP.

In conclusion, triplet phenylarsinidene was successfully generated in cryogenic matrices and was spectroscopically characterized by means of IR and UV/Vis spectroscopy. Doping matrices of phenylarsinidene with molecular oxygen led to oxidation to *anti*-phenyldioxylarsinene, with reactivity

different from that of phenylphosphinidene and phenylnitrene with oxygen. Dioxophenylarsine, the arsenic analogue of nitrobenzene, was obtained through subsequent irradiation. Our disclosure of a straightforward preparation of phenylarsinidine contributes to our knowledge of fundamental chemistry of a higher pnictogen sextet species and provides new entry points for the use of arsinidenes in synthetic and materials chemistry.

References

1. Bourissou, D., Guerret, O., Gabbaï, F.P. & Bertrand, G. Stable Carbenes. *Chem. Rev.* **100**, 39-92 (2000).
2. Sander, W., Bucher, G. & Wierlacher, S. Carbenes in matrixes: spectroscopy, structure, and reactivity. *Chem. Rev.* **93**, 1583-1621 (1993).
3. Hirai, K., Itoh, T. & Tomioka, H. Persistent Triplet Carbenes. *Chem. Rev.* **109**, 3275-3332 (2009).
4. Dielmann, F. et al. A Crystalline Singlet Phosphinonitrene: A Nitrogen Atom-Transfer Agent. *Science* **337**, 1526-1528 (2012).
5. Wentrup, C. Carbenes and Nitrenes: Recent Developments in Fundamental Chemistry. *Angew. Chem. Int. Ed.* **57**, 11508-11521 (2018).
6. Sun, J. et al. A platinum(ii) metallonitrene with a triplet ground state. *Nat. Chem.* **12**, 1054-1059 (2020).
7. Hinz, A., Hansmann, M.M., Bertrand, G. & Goicoechea, J.M. Intercepting a Transient Phosphino-Arsinidene. *Chem. Eur. J.* **24**, 9514-9519 (2018).
8. Yao, S. et al. Facile Access to NaOC≡As and Its Use as an Arsenic Source To Form Germylidenylarsinidene Complexes. *Angew. Chem. Int. Ed.* **56**, 7465-7469 (2017).
9. Dixon, R.N. & Lamberton, H.M. The A, $^{3}\Pi_{i}-X,\ ^{3-}$ band systems of AsH and AsD. *J. Mol. Spectrosc.* **25**, 12-33 (1968).
10. Arens, M. & Richter, W. Spectroscopic observation of the $b\,^{1}\Sigma^{+}\rightarrow\tilde{X}\,^{3}\Sigma^{-}$ transition of AsH. *J. Chem. Phys.* **93**, 7094-7096 (1990).
11. Berkowitz, J. Photoionization mass spectrometric studies of AsH_n (n=1–3). *J. Chem. Phys.* **89**, 7065-7076 (1988).
12. Hensel, K.D., Hughes, R.A. & Brown, J.M. IR spectrum of the AsH radical in its $X\ ^{3}\Sigma^{-}$ state, recorded by laser magnetic resonance. *J. Chem. Soc., Faraday Trans.* **91**, 2999-3004 (1995).
13. Sharma, M.K., Neumann, B., Stammler, H.-G., Andrada, D.M. & Ghadwal, R.S. Electrophilic terminal arsinidene-iron(0) complexes with a two-coordinated arsenic atom. *Chem. Commun.* **55**, 14669-14672 (2019).
14. Fischer, M., Reiß, F. & Hering-Junghans, C. Titanocene pnictinidene complexes. *Chem. Commun.* **57**, 5626-5629 (2021).
15. Bonanno, J.B., Wolczanski, P.T. & Lobkovsky, E.B. Arsinidene, Phosphinidene, and Imide Formation via 1,2-H2-Elimination from (silox)3HTaEHPh (E = N, P, As): Structures of (silox)3Ta:EPh (E = P, As). *J. Am. Chem. Soc.* **116**, 11159-11160 (1994).
16. Wildman, E.P., Balázs, G., Wooles, A.J., Scheer, M. & Liddle, S.T. Triamidoamine thorium-arsenic complexes with parent arsenide, arsinidiide and arsenido structural motifs. *Nat. Commun.* **8**, 14769 (2017).
17. Pugh, T., Kerridge, A. & Layfield, R.A. Yttrium Complexes of Arsine, Arsenide, and Arsinidene Ligands. *Angew. Chem. Int. Ed.* **54**, 4255-4258 (2015).
18. Arduengo, A.J. et al. Carbene−Pnictinidene Adducts. *Inorg. Chem.* **36**, 2151-2158 (1997).
19. Doddi, A. et al. N-Heterocyclic carbene-stabilised arsinidene (AsH). *Chem. Commun.* **53**, 6069-6072 (2017).
20. Präsang, C., Stoelzel, M., Inoue, S., Meltzer, A. & Driess, M. Metal-Free Activation of EH3 (E=P, As) by an Ylide-like Silylene and Formation of a Donor-Stabilized Arsasilene with a HSi=AsH Subunit. *Angew. Chem. Int. Ed.* **49**, 10002-10005 (2010).
21. Andrews, L. & Cho, H.-G. Matrix Infrared Spectra and Quantum Chemical Calculations of Ti, Zr, and Hf Dihydride Phosphinidene and Arsinidene Molecules. *Inorg. Chem.* **55**, 8786-8793 (2016).

22. Zhang, L., Dong, J. & Zhou, M. Formation and characterization of the AsCO and AsCO− molecules. A matrix isolation FTIR and theoretical study. *Chem. Phys. Lett.* **335**, 334-338 (2001).
23. Green, J.P. et al. An Air-Stable Semiconducting Polymer Containing Dithieno[3,2-b:2′,3′-d]arsole *Angew. Chem. Int. Ed.* **55**, 7148-7151 (2016).
24. Fischer, M. et al. Isolable Phospha- and Arsaalumenes. *J. Am. Chem. Soc.* **143**, 4106-4111 (2021).
25. Lloyd, N.C., Morgan, H.W., Nicholson, B.K. & Ronimus, R.S. The Composition of Ehrlich's Salvarsan: Resolution of a Century-Old Debate. *Angew. Chem. Int. Ed.* **44**, 941-944 (2005).
26. Smith, R.C., Gantzel, P., Rheingold, A.L. & Protasiewicz, J.D. Arsa-Wittig Complexes (ArAsPMe3) as Intermediates to Diarsenes. *Organometallics* **23**, 5124-5126 (2004).
27. Weber, L. The chemistry of diphosphenes and their heavy congeners: synthesis, structure, and reactivity. *Chem. Rev.* **92**, 1839-1906 (1992).
28. Qian, W. et al. Vibrational spectrum and photochemistry of phosphaketene HPCO. *Phys. Chem. Chem. Phys.* **23**, 19237-19243 (2021).
29. Chu, X. et al. Methoxyphosphinidene and Isomeric Methylphosphinidene Oxide. *J. Am. Chem. Soc.* **140**, 13604-13608 (2018).
30. Mardyukov, A., Niedek, D. & Schreiner, P.R. Preparation and Characterization of Parent Phenylphosphinidene and Its Oxidation to Phenyldioxophosphorane: The Elusive Phosphorus Analogue of Nitrobenzene. *J. Am. Chem. Soc.* **139**, 5019-5022 (2017).
31. Mardyukov, A. & Niedek, D. Photochemical reactions of triplet phenylphosphinidene with carbon monoxide and nitric oxide. *Chem. Commun.* **54**, 13694-13697 (2018).
32. Bucher, G. et al. Infrared, UV/Vis, and W-band EPR spectroscopic characterization and photochemistry of triplet mesitylphosphinidene. *Angew. Chem., Int. Ed.* **44**, 3289-3293 (2005).
33. Akimov, A.V., Ganushevich, Y.S., Korchagin, D.V., Miluykov, V.A. & Misochko, E.Y. The EPR Spectrum of Triplet Mesitylphosphinidene: Reassignment and New Assignment. *Angew. Chem., Int. Ed.* **56**, 7944-7947 (2017).
34. Lawzer, A.-L., Custer, T., Guillemin, J.-C. & Kołos, R. An Efficient Photochemical Route Towards Triplet Ethynylphosphinidene, HCCP. *Angew. Chem. Int. Ed.* **60**, 6400-6402 (2021).
35. Liu, L., Ruiz, David A., Munz, D. & Bertrand, G. A Singlet Phosphinidene Stable at Room Temperature. *Chem* **1**, 147-153 (2016).
36. Transue, W.J. et al. Mechanism and Scope of Phosphinidene Transfer from Dibenzo-7-phosphanorbornadiene Compounds. *J. Am. Chem. Soc.* **139**, 10822-10831 (2017).
37. Mardyukov, A., Keul, F. & Schreiner, P.R. Isolation and Characterization of the Free Phenylphosphinidene Chalcogenides $C_6H_5P{=}O$ and $C_6H_5P{=}S$, the Phosphorous Analogues of Nitrosobenzene and Thionitrosobenzene. *Angew. Chem., Int. Ed.* **59**, 12445-12449 (2020).
38. Zhao, X. et al. Phosphorus Analogues of Methyl Nitrite and Nitromethane: CH_3OPO and CH_3PO_2. *Angew. Chem., Int. Ed.* **58**, 12164-12169 (2019).
39. Lee, T.J. & Taylor, P.R. A diagnostic for determining the quality of single-reference electron correlation methods. *Int. J. Quantum Chem.* **36**, 199-207 (1989).
40. Mieres-Perez, J., Mendez-Vega, E., Velappan, K. & Sander, W. Reaction of Triplet Phenylnitrene with Molecular Oxygen. *J. Org. Chem.* **80**, 11926-11931 (2015).

Additional information

All data is available in the main text or the supplementary information. The supplementary information includes: IR and UV/Vis spectra, NMR spectra, IR table, Cartesian coordinates, absolute energies of all optimized geometries, experimental procedures and simulations (PDF).

Competing interests

The authors declare no competing financial interest.

Acknowledgements

Financial support by the Deutsche Forschungsgemeinschaft (DFG) *via* the grant MA 8773/3-1 is gratefully acknowledged.

Methods

Matrix Apparatus Design. For the matrix isolation studies, we used an APD Cryogenics HC-2 cryostat with a closed-cycle refrigerator system, equipped with an inner CsI window for IR measurements. Spectra were recorded with a Bruker Vertex 70 FT-IR spectrometer with a spectral range of 4000−400 cm^{-1} and a resolution of 0.7 cm^{-1} and UV/Vis spectra were recorded with a JASCO V-670 spectrophotometer equipped with an inner sapphire window. A high-pressure mercury lamp (HBO 200, Osram) with a monochromator (Bausch & Lomb) was used for irradiation. For the combination of high-vacuum flash pyrolysis with matrix isolation, we employed a small, homebuilt, water-cooled oven, which was directly connected to the vacuum shroud of the cryostat. The pyrolysis zone consisted of an empty quartz tube with an inner diameter of 8 mm, which was resistively heated over a length of 50 mm by a coaxial wire. The temperature was monitored with a NiCr−Ni thermocouple. Azides were evaporated (2: 20 °C) from a storage bulb into the quartz pyrolysis tube. At a distance of approximately 50 mm, all pyrolysis products were co-condensed with a large excess of argon (typically 60−120 mbar from a 2000 mL storage bulb) on the surface of the matrix window at 10 K.

Caution*! Arsenic compounds are hazardous toxic and harmful to the environment, which should be handled with careful protection and all trash should be disposed of specially. Covalent azides are potentially hazardous explosives. Although we have not experienced any incident during this work, it should be handled with great care in small quantities (< 5 mmol) under oxygen- and water-free conditions, and safety precautions (face shields, Kevlar gloves, and protective leather clothing) are recommended. Any contact with metal should be avoided for the sample.*

Synthesis of phenyldiazidoarsine 2. In a flame-dried Schlenk flask, 0.13 g (0.20 mmol) activated NaN_3[1] were suspended in 0.80 mL anhydrous CH_3CN and 7.00 μL (ca. 0.05 mmol) freshly distilled phenyldichloroarsine was added.[2] The mixture was stirred for 12 h at room temperature. Filteration afforded a colorless solution. Then it was cooled to 0 °C and brought to reduced pressure to remove solvent to leave a white solid. Quantitative yields were typically obtained. The purity of the sample was confirmed by NMR (^{1}H NMR (400 MHz, CD_3CN): δ = 7.89 (m, 2 H), 7.68 (m, 3 H). $^{13}C\{^1H\}$ NMR (162 MHz, CD_3CN): δ = 132.20, 131.50, 130.9, 130.45, 129.79, 129.58 ppm. Figure S6, Figure S7).

Computations. Geometry optimizations at CCSD(T)/cc-pVTZ[3-7] level and minimum energy crossing-point (MECP) searching were performed by ORCA 5.0.[8] B3LYP[9,10] and CASSCF[11,12]

computations were carried out by Gaussian16 program[13] with def2-TZVP and cc-pVDZ basis set.[14] Local minima were confirmed by vibrational frequencies analysis, and transition states were further confirmed by intrinsic reaction coordinate (IRC) calculations. Wavefunction analysis results were obtained from Multiwfn 3.8.[15] Natural bond order and resonance structures were computed by NBO 7.0.[16]

Supplementary References

1. Pople, J.A., Head- Gordon, M. & Raghavachari, K. Quadratic configuration interaction. A general technique for determining electron correlation energies. *J. Chem. Phys.* **87**, 5968-5975 (1987).
2. Klapötke, T.M. & Geissler, P. Preparation and characterization of the first binary arsenic azide species: $As(N_3)_3$ and $[As(N_3)_4][AsF_6]$. *J. Chem. Soc., Dalton Trans.*, 3365-3366 (1995).
3. Gericke, R. & Wagler, J. (2-Pyridyloxy)arsines as ligands in transition metal chemistry: a stepwise As(iii) → As(ii) → As(i) reduction. *Dalton Trans.* **49**, 10042-10051 (2020).
4. Bartlett, R.J. & Purvis, G.D. Many-body perturbation theory, coupled-pair many-electron theory, and the importance of quadruple excitations for the correlation problem. *Int. J. Quantum Chem.* **14**, 561-581 (1978).
5. Pople, J.A., Krishnan, R., Schlegel, H.B. & Binkley, J.S. Electron correlation theories and their application to the study of simple reaction potential surfaces. *Int. J. Quantum Chem.* **14**, 545-560 (1978).
6. Jr., T.H.D. Gaussian basis sets for use in correlated molecular calculations. I. The atoms boron through neon and hydrogen. *J. Chem. Phys.* **90**, 1007-1023 (1989).
7. Woon, D.E. & Jr., T.H.D. Gaussian basis sets for use in correlated molecular calculations. III. The atoms aluminum through argon. *J. Chem. Phys.* **98**, 1358-1371 (1993).
8. Neese, F. Software update: The ORCA program system—Version 5.0. *Wiley Interdiscip. Rev.: Comput. Mol. Sci.* **12**, e1606 (2022).
9. Becke, A.D. Density- functional thermochemistry. III. The role of exact exchange. *J. Chem. Phys.* **98**, 5648-5652 (1993).
10. Stephens, P.J., Devlin, F.J., Chabalowski, C.F. & Frisch, M.J. Ab Initio Calculation of Vibrational Absorption and Circular Dichroism Spectra Using Density Functional Force Fields. *J. Phys. Chem.* **98**, 11623-11627 (1994).
11. Roos, B.O. The Complete Active Space Self-Consistent Field Method and its Applications in Electronic Structure Calculations. in *Adv. Chem. Phys.* 399-445 (1987).
12. Roos, B.O. The complete active space SCF method in a fock-matrix-based super-CI formulation. *Int. J. Quantum Chem. Symp.* **18**, 175-189 (1980).
13. Frisch, M.J. et al. *Gaussian 16 Rev. B.01 Inc., Wallingford CT* (2016).
14. Weigend, F. & Ahlrichs, R. Balanced basis sets of split valence, triple zeta valence and quadruple zeta valence quality for H to Rn: Design and assessment of accuracy. *Phys. Chem. Chem. Phys.* **7**, 3297-305 (2005).
15. Lu, T. & Chen, F. Multiwfn: A multifunctional wavefunction analyzer. *J. Comput. Chem.* **33**, 580-592 (2012).
16. Glendening, E.D. et al. NBO 7.0. (2018).